

# Predictions of the Hydrodynamic Performance of Horizontal Axis Marine Current Turbines Using a Panel Method Program

Mahrez Ait-Mohammed<sup>1</sup>, Mostapha Tarfaoui<sup>1</sup> and Jean Marc Laurens<sup>1</sup>

<sup>1</sup> Department of Fluid Dynamics, Materials and Structures  
 ENSTA Bretagne – LBMS, 29806 Brest (France)

Phone number: +33(0) 298348713, e-mail: mahrez.ait\_mohammed@ensta-bretagne.fr

Phone number: +33(0) 298348705, e-mail: mostapha.tarfaoui@ensta-bretagne.fr

Phone number: +33(0) 298348752, e-mail: jean.marc\_laurens@ensta-bretagne.fr

## Abstract.

The marine current turbine is the mechanical device that captures the kinetic energy of marine current to generate electrical power. This paper presents the application of an academic panel code based on potential flow theory for the analysis of marine current turbines. The aim of this work is also to analyze the effect of the addition of a duct on the hydrodynamic performance of the turbine. The numerical results show that the addition of duct improves significantly the efficiency of the turbine.

## Keywords

Marine Current Turbines, Panel Method, Boundary Element Method, Turbine Design, Performances Predictions, Ducted turbine.

## 1. Introduction

The kinetic energy available within tidal currents is an untapped source of renewable energy. If an effective method of capturing this energy can be developed, tidal currents could be harnessed to help satisfy the world's growing energy needs. Horizontal axis marine current turbines are one promising technology that is being developed for this purpose [1].

Various global studies have shown that marine currents have a large potential as a predictable sustainable resource for commercial scale generation of electrical power.

There has been a growing interest in the use of marine current turbines for electrical power production. The ability to predict the hydrodynamic performance of marine current turbines is essential for the design and analysis of such systems.

The performance of marine current turbines is often expressed by the power coefficient ( $C_p$ ). There is a limit output of one-dimensional Betz model initially applied for turbine with horizontal axis, indicating that the power coefficient value cannot exceed 16/27. This means that the turbine cannot extract more than 59.3% of the energy contained in the flow. Gorban et al. [2] also redefined the Betz theory limit taking into account the deflection of the streamlines passing through the rotor (figure 1).

This new approach, called GGS model by the authors, indicates a limit of 30.1% for horizontal axis turbines. As we will show later in this paper, this lower limit has been established using a model that cannot be applied for marine current turbines.

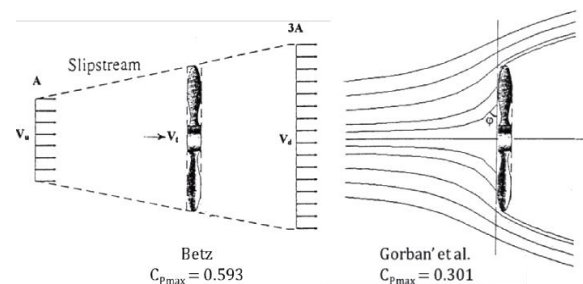


Fig.1. Comparison between the Betz limit and the GGS limit [2].

Regardless of the adopted limit, it is impossible to extract all the hydrokinetic energy contained in the flow. However it is possible to improve the hydrodynamic performance in terms of power coefficient of a bare turbine (without duct) by installing a duct. There has been considerable effort and discussion in the literature concerning the addition of a duct to wind/water turbines to extract more power than a bare turbine [3], i.e. to surpass the theoretical power extraction limit defined by Betz and Gorban et al [2] for horizontal axis turbines. In this context, the introduction of duct systems increase significantly the performance of such turbines.

This paper presents the application of an academic panel code based on potential flow theory to the analysis of marine current turbines. In theory this code has been developed for the hydrodynamic analysis of marine propellers. However, to extrapolate the results in propeller format corresponding to a marine current turbine, three important variables need to be correlated. They are the advance coefficient ( $J$ ) versus tip speed ratio ( $TSR$ ), thrust coefficient ( $K_t$ ) versus turbine thrust coefficient ( $C_t$ ) and torque coefficient ( $K_q$ ) versus turbine power coefficient ( $C_p$ ). When the ( $K_t$ ) and the ( $K_q$ ) are obtained, versus ( $J$ ) from the panel method code, they can be represented as ( $C_t$ ) and ( $C_p$ ) for turbine as a function of tip speed ratio ( $TSR$ ). With the definitions of propeller

advance coefficient,  $J = V_0/nD$ , propeller thrust coefficient  $K_t = T/\rho n^2 D^4$ , propeller torque coefficient  $K_q = Q/\rho n^2 D^5$ , turbine tip speed ratio  $TSR = \omega R/V_0$ , turbine thrust coefficient  $C_t = T/\frac{1}{2}\rho AV_0^2$ , and turbine power coefficient  $C_p = Q\omega/\frac{1}{2}\rho AV_0^3$ , the three parameters for marine current turbines in terms of propellers are:

$$TSR = \frac{\omega R}{V_0} = \frac{2\pi n R}{V_0} = \frac{\pi n D}{V_0} = \frac{\pi}{J} \quad (1)$$

$$C_t = \frac{T}{\frac{1}{2}\rho AV_0^2} = \frac{K_t \rho n^2 D^4}{\frac{1}{2}\rho \frac{\pi D^2}{4} V_0^2} = \frac{8K_t}{\pi J^2} \quad (2)$$

And

$$C_p = \frac{Q\omega}{\frac{1}{2}\rho AV_0^3} = \frac{K_q \rho n^2 D^5}{\frac{1}{2}\rho \frac{\pi D^2}{4} V_0^3} = \frac{16K_q n^3 D^3}{V_0^3} = \frac{16K_q}{J^3} \quad (3)$$

## 2. Theory, Models and Numerical Methods

The panel methods are based on potential flow theory. The potential flow model is derived from the Navier-Stokes model as follows:

We first consider an incompressible ( $\rho = cst$ ) and Newtonian fluid ( $\mu = cst$ ). Applying the principle of mass conservation, we obtain:

$$\text{div}(\vec{V}) = 0 \quad (4)$$

Where  $\vec{V}$  is the velocity vector.

Applying the second Newton law, if gravity is ignored, we obtain:

$$\rho \cdot \frac{D\vec{V}}{Dt} = -\vec{\nabla}P + \mu \cdot \vec{\Delta}\vec{V} \quad (5)$$

Where the left term is the substantial (or total) derivative of the velocity vector multiplied by the density,  $p$  is the pressure, and  $\mu$  is the fluid molecular viscosity.

Equations (4) and (5) are the Navier-Stokes equations for an incompressible and Newtonian fluid. We now assume that the fluid is inviscid ( $\mu = 0$ ), and the flow is non rotational  $\text{rot}\vec{V} = 0$ . This last assumption is equivalent to state that a potential function  $\varphi$  exists such as  $\vec{V} = \vec{\Delta}\varphi$ . With these assumptions, equation (5) becomes the Bernoulli equation and equation (4) becomes the Laplace equation for  $\varphi$ :

$$\Delta\varphi = 0 \quad (6)$$

Solving the potential flow is therefore to find a potential function  $\varphi$  which satisfies the Laplace equation. The velocities are derived from the potential function since,  $\vec{V} = \vec{\Delta}\varphi$ , and the pressure is computed from the Bernoulli equation which is true everywhere in the fluid for a potential flow.

From there, the panel methods consist in placing singularities such as dipoles (or doublets) and sources on the surface of the obstacles. The singularities are particular solutions of the Laplace equation and their intensities are computed to fit the boundary conditions. For a non-lifting body, the only boundary condition is a slip condition at its surface. For a lifting body such as a wing, the slip condition is not sufficient since theoretically, a body in an inviscid fluid flow does not produce any hydrodynamic forces. To mimic the behavior of viscous fluid flow around a lifting body, an additional condition is also required. It consists in forcing the flow to be lined up with the trailing edge. This boundary condition is known as the Kutta-Joukowski condition and in practice it only can be applied for bodies presenting a sharp trailing edge. Once the intensities of the singularities have been computed respecting the boundary conditions, we can compute the velocities and the pressure anywhere in the fluid domain.

The panel method code we use belongs to what Hoeijmakers, H.W.M.; [4] refers to as "second generation" panel methods involving the Dirichlet condition ( $\varphi = 0$  in the inner body). Body surfaces are discretized into first order panels carrying constant source and doublet distributions. The wake developing behind the rotor is formed with a sheet of first order panels carrying constant doublet distributions and it is generated with time in a Lagrangian manner. Thanks to the Dirichlet condition, imposing the slip condition on the body surface, determines the sources directly from the inlet velocity and the normal vectors. Hence, the unknown of the problem are the dipoles. The locations of the sheet panels vertices are recalculated at each time step but not the dipoles they carry. Non-lifting bodies such as the hub are discretised using first order panels carrying constant source and dipole distributions. The rotor hub can be easily modelled this way but in most cases it does not influence the hydrodynamic coefficients so in the results presented here, we do not simulate its presence. The code allows for unsteady state flow simulation and the body thickness representation leads to an accurate distribution of pressure coefficients ( $C_p$ ) on duct and blades surfaces. From the velocities, we compute the local Reynolds number,  $R_n$ , on each surface panel which gives us the local friction coefficient  $C_f$  using standard formulae:

$$0.027/\sqrt[7]{R_n} \text{ for turbulent flow and } 0.664/\sqrt{R_n} \text{ for laminar}$$

flow. The transition is forced at  $R_n = 5 \cdot 10^5$ .

The panel method only requires a surface mesh of the solid objects. We developed a friendly user mesh generator for the blades and duct surfaces. A typical configuration is presented in Figure 2. In this example, we also show the wake which has been automatically generated by the potential flow code. Since the rotor blades and the duct are computed as lifting bodies, they must present a sharp trailing edge from which the wake modelled as a sheet of first order panels carrying constant doublet distributions originates.

The procedure consists in separating the flow around the

rotor and the flow around the duct into two different runs. Once the flow around the duct has been solved, we compute the duct induced velocities at the blades control points (i.e. the centers of all panels). The flow around the rotor is then computed in the presence of the duct induced velocities. We then compute the rotor induced velocities on the surface of the duct. The procedure is repeated until convergence which occurs after only a few iterations [5].

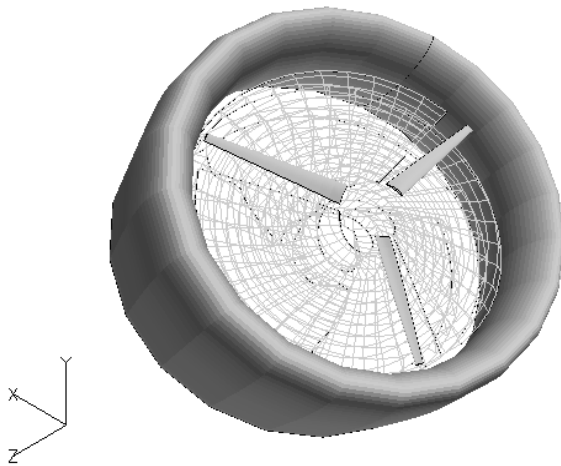


Fig.2. Example of ducted water turbine. The wake behind the blades is generated by the computation

### 3. Numerical Methods

#### A. Model Turbine

The turbine rotor described and tested by Bahaj et al. [6] is considered. For this rotor a considerable set of experimental data obtained from cavitation tunnel and towing tank tests is available in the literature [6]. The turbine is a three-bladed turbine with NACA 63-415 sections. The standard geometry has a pitch angle at the blade root equal to 15°, corresponding to a 0° set angle, the blade set angle is the angle at the tip of the blade (pitch). In the present work, 0°, 5°, 10° and 13° blade set angle were considered. The rotor hub can be easily modelled but in most cases it does not influence the hydrodynamic coefficients so in the results presented here, we do not simulate its presence.

A view of the blade mesh and the turbine rotor geometry is shown in figure 3.

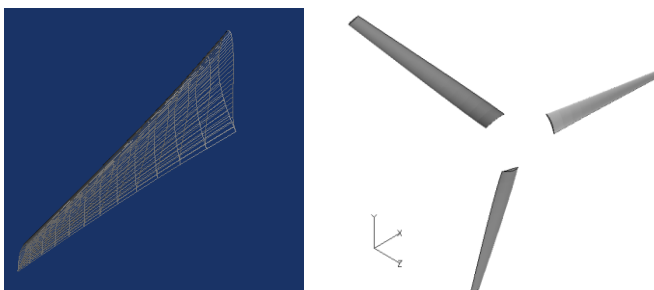


Fig.3. Design of blade with NACA 63-415 and 0° set angle

The lift and drag coefficients curves for the NACA 63-415 profile computed with XFOil are presented on Figure 4. It clearly appears that a severe flow separation occurs after 6°.

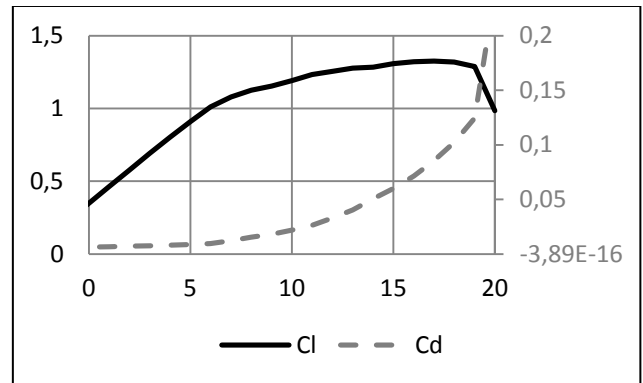


Fig.4. Lift and Drag coefficients versus the angle of attack for the NACA 63-415 section as computed with XFOil

#### B. Performance comparison between theory and data experiments

The results of the performance of the model turbine from boundary element method (panel method code) in flow speed at  $V_0 = 1.8 \text{ m/s}$  has been compared with the experimental data [6] at blade set angles of 0°, 5°, 10° and 13°. Figures 5 to 8 show a comparison of the numerical and analytical power coefficient  $C_p$  with the experimental data. The analytical expression of the power coefficient is given by Werle et al. [3]:

$$C_p = \frac{1}{2}(1 + C_s)C_t[1 + \sqrt{1 - C_t}] \quad (7)$$

Where  $C_s$  is the duct drag coefficient and  $C_t$  is the rotor thrust coefficient. In the case of un-ducted turbine, the duct drag coefficient  $C_s$  is equal to zero.

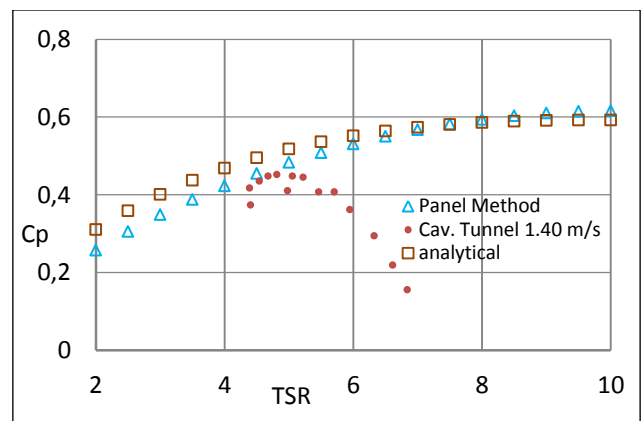


Fig.5. Comparison of power coefficient  $C_p$  predicted by Panel code at 0° set angle with experimental data

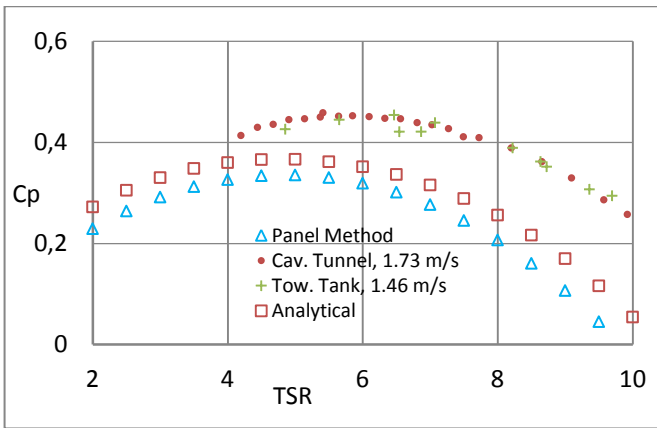


Fig.6. Comparison of power coefficient  $C_p$  predicted by Panel code at  $5^\circ$  set angle with experimental data

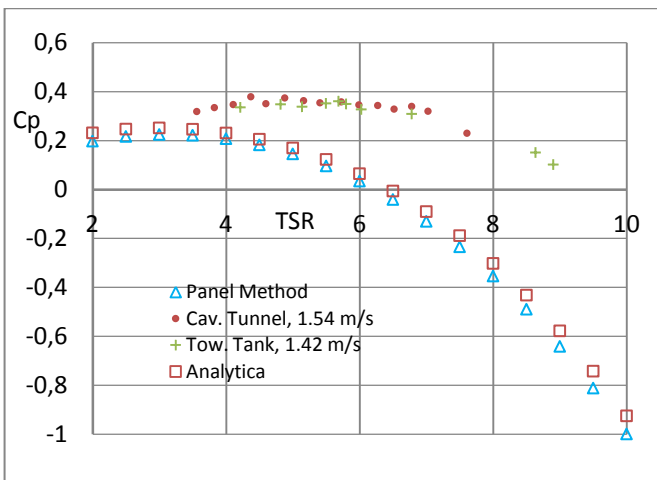


Fig.7. Comparison of power coefficient  $C_p$  predicted by Panel code at  $10^\circ$  set angle with experimental data

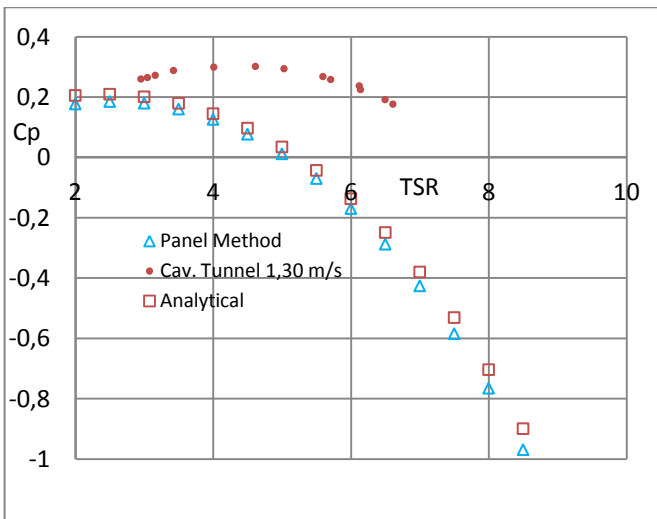


Fig.8. Comparison of power coefficient  $C_p$  predicted by Panel code with  $13^\circ$  set angle rotor and the experimental data

### C. Discussion

Examining the four rotor set angles, we note that the best performance ( $C_p$  lower than measurements data) was obtained for a  $5^\circ$  set angle corresponding to a  $20^\circ$  root pitch. It is also noted that the maximum numerical power coefficient attains a maximum value of about 0.34 at  $TSR = 5$ . See Figure 6. The analytical model of Werle et

al. [3] is slightly pessimistic but follows the tendencies indicated by the experimental results. The panel method code, although more accurate, gives some even lower  $C_p$  values. Baltazar and Falcao de Campos. [8] obtained some similar results with an equivalent method. They introduced a refinement to their model to adjust the drag. When they only take the friction into account, as we do, they obtain the same results we do. They also adjust the drag to include all viscous effects including flow separation. With this latter correction, they get much closer to the experimental results but it requires 2D sections XFOIL analysis. The ultimate tool would be to use a Navier-Stokes solver with a proper turbulence model as in Afgan et al. [9] who obtained results very close to the experimental results of Bahaj et al. [6]. All this proves that even when the turbine operates within its high  $C_p$  range, some flow separation occurs.

Before we discuss the flow separation in more detail, we must underline the fact that all the results, experimental and numerical, predict a  $C_p$  well over the limit of 30.1% given by the GGS model [2]. Examining this paper in more detail, we found out that it is based assuming Darcy's law which only applies for Stokes' flows. Surprisingly this paper has been cited over 150 times (according the Google Scholar) but this inconsistency has never been highlighted. Only McNaughton [10] in his voluminous report has indicated that the GGS model was probably wrong.

The discrepancy between the panel method code results and the experimental results are essentially due to the fact that potential flow code cannot simulate flow separation. In Figures 7 and 8 the differences between our model and the experiment are even more important. In these cases the set angles are  $10^\circ$  and  $13^\circ$  which correspond to  $25^\circ$  and  $28^\circ$  root pitch angles respectively. These pitch angles lead the poorest hydrodynamic efficiency curves because the blades are in propulsion mode (angle of attack is negative). This is in full consistent with the results of the literature [6] and [11]. Figure 5 presents the comparative results for the lowest pitch angle. The numerical results are closer to the experimental results, until flow separation occurs at  $TSR = 5$ .

To illustrate the flow separation occurrence, Figure 9 presents the sections angles of attack from blade root to tip when the set angle is  $13^\circ$ . As can be seen, in most cases, the angle of attack reaches high values. Referring to Abbott and Von Doenhoff [12], all 2D symmetrical foil approaches the stall at  $15^\circ$  angle of attack. With the NACA63415, flow separation occurs even earlier. Although 3D effects reduce the apparent angle of attack, the values presented in Figure 9, are such that separation occurs for all configuration at least at the blade root. The separation and stall cannot be simulated with the panel method code. However, as for a propeller, it is not advisable to operate a water turbine in a flow separation condition. In other word, the best configuration for the present turbine is the  $5^\circ$  blade set angle at  $TSR = 5$ .

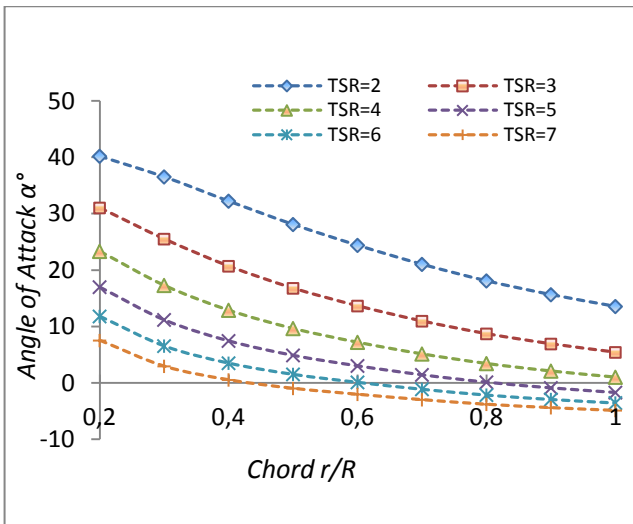


Fig.9. angle of attack versus chord of 13° set angle

#### 4. Ducted Turbine

Augmentation channels induce a sub-reference pressure within a constrained area and thereby increase the flow velocity. If a turbine is placed in such a channel, the flow velocity around the rotor is higher than the current velocity. Since the potential power is proportional to the cube of the inlet velocity, the expected gain can be very important.

These structures are fixed at the periphery of the rotor to increase the power extracted by the marine current turbine, geometry of marine current turbines facilitates the introduction of this type of device. These systems create a funnelling effect which increases the flow through the rotor. Drag exerted by the fluid on the duct is translating on a depression at the output of the duct which is at the origin of the suction phenomenon [13].

Figure 10 shows the evolution of the power coefficient as a function of the rotor drag coefficient and the duct drag coefficient. The analytical expression of the power coefficient  $C_p$  in the presence of a duct is the equation (7).

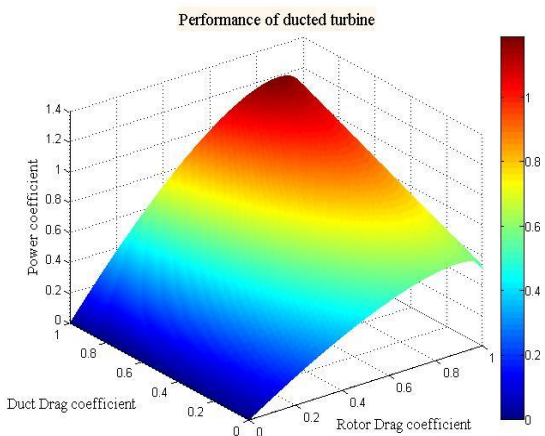


Fig.10. Evolution of the power coefficient as function of the rotor drag coefficient and the duct drag coefficient

In addition, the aim of this work is also to analyze the effect of a 0.950 m diameter and 0.4m chord duct with

NACA 4-Digit profile on the hydrodynamic performance of the turbine with 5° set angle rotor.

Several axial positions of the rotor to the inner of the duct were tested and the numerical results with panel method showed that it is at 25% of the duct chord from the leading edge where we find the best efficiency.

Figure 11 illustrate the duct surface pressure coefficient distribution at maximum power extraction, according to  $C_p = 0.94$  at  $TSR = 7.5$ .

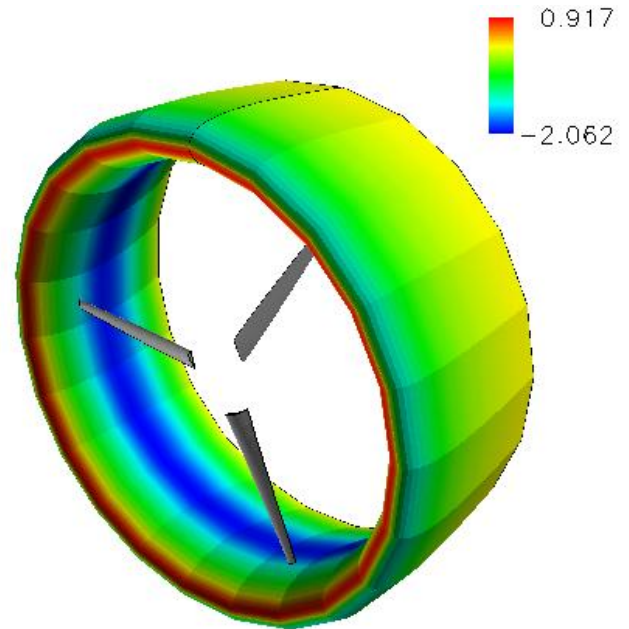


Fig.11. Distribution of the pressure coefficient on the duct at  $TSR=7.5$

Figure 12 shows the evolution of the power coefficient  $C_p$  of the ducted turbine with a NACA4424 profile and the bare turbine with 0.950m rotor diameter. The numerical results show, for the same overall area, that the ducted turbine produces more power than the bare turbine. The  $TSR$  are not the same since the action of the duct shifts the advance parameter ( $C_p = 0.94$  at  $TSR = 7.5$  versus  $C_p = 0.35$  at  $TSR = 5$ ). If these findings are confirmed, it means that it is advisable to install water turbines equipped with a duct.

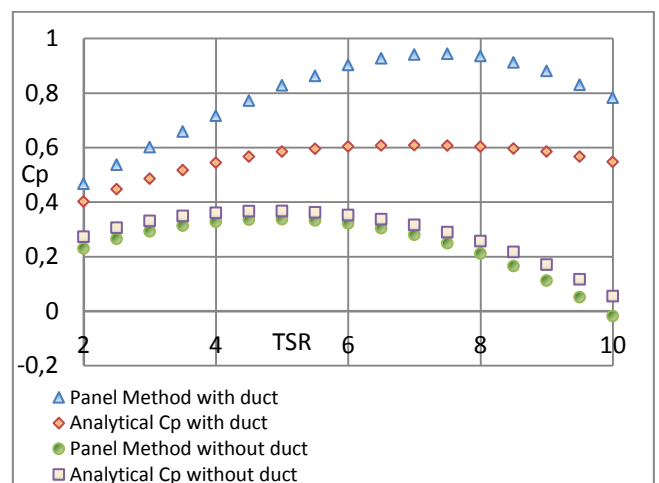


Fig.12. Comparison of power coefficient  $C_p$  predicted by Panel Method between ducted and un-ducted turbine for the same overall

## Conclusion and future work

An academic panel code based on potential flow theory has been used to assess the hydrodynamic performance of a marine current turbine with and without a duct. The numerical results for the bare turbine have been compared with the experimental results reported in reference [6]. Although the trend is the same, the numerical results present significantly lower values for the power coefficient. Baltazar and Falcao de Campos [8] obtained the same results with a very similar method and they propose to correct the section drag to account for flow separation. From the spanwise distribution of sections angles, it appears that flow separation must occur even for configurations with high power coefficient values. Flow separation and cavitation being closely linked, serious investigation has to be carried out to decide whether it is advisable to design a water turbine presenting flow separation even in normal operational mode. Simulations with a Navier-Stokes solver are needed as long as the turbulence model is capable of predicting the correct hydrodynamic forces in presence of flow separation which is known to be a challenging problem. Experimental results with flow separation monitoring are also needed.

In the course of our study, we questioned the upper limit given by the GGS model [2] which is half the Betz limit. We found that the GGS model is based on a wrong assumption and serious contradiction are embedded in the proof. Surprisingly the paper has been cited more than a hundred times and only one author suspected something was wrong and no one investigated any further.

Finally, the results of our simulations with the presence of a duct show that the addition of this appendix produces a very significant increase in power outlet with a same overall area.

The arguments given against the addition of a duct are usually coming from the structural point of view. Our future line of investigation will therefore concern the material and structure behaviour of the ducted water turbine.

## Acknowledgement

We would like to thank “Brest Métropole Océane” for their financial support for this research work.

## References

- [1] P. Fraenkel, “Power From Marine Current, Proceedings of the Institution of Mechanical Engineers”, Part A: Journal of Power and energy, 2002, pp. 1-14.
- [2] A. N. Gorban, A. M. Gorlov and V. M. Silantyev, “Limits of the Turbines Efficiency for Free Fluid Flow”, Journal of Energy Resources Technology. 2001, Vol. 123, pp. 311-312.
- [3] M. J. Werle, and W. M. Presz, “Ducted Wind/Water Turbines and Propellers Revisited”, Journal of Propulsion and Power. 2008, Vol. 24, pp. 1146-1150.
- [4] H. W. M. Hoeijmakers, “Panel Methods for Aerodynamic Analysis and Design”, AGARD Report 783. 1992, pp. 5.1-5.47.
- [5] J. M. Laurens, S. Moyne and F. Deniset, “A BEM Method for the Hydrodynamic Analysis of Fishing Boats Propulsive Systems”, in Proc. ISFVEE 2012, pp.1-7.
- [6] A.S. Bahaj, W. M. J. Batten, G. McCann, “Experimental Verifications of Numerical Predictions for the Hydrodynamic Performance of Horizontal Axis Marine Current Turbines”, Renewable Energy. 2007, Vol. 32, pp. 2479-2490
- [7] W. M. J. Batten, A. S. Bahaj, A. F. Molland, J. R. Chaplin, “Experimentally Validated Numerical Method for The Hydrodynamic Design of Horizontal Axis Tidal Turbines”, Ocean Engineering. 2006, Vol. 34, pp. 1013-1020.
- [8] J. Baltazar, J. A. C. Falcão de Campos, “Unsteady Analysis of a Horizontal Axis Marine Current Turbine in Yawed Inflow Conditions with a Panel Method”, in Proc. SMP2009, pp.1-9.
- [9] I. Afgan, J. McNaughton, S. Rolfo, D. D. Apsley, T. Stallard, and P. Stansby, “Turbulent Flow and Loading on a Tidal Stream Turbine by LES and RANS”, International Journal of Heat and Fluid Flow. 2013, Vol 43, pp.96-108.
- [10] J. McNaughton, “Turbulence Modelling in the Near-Field of an Axial flow Tidal Turbine in Code-Saturne”, First Year Report, 2010, pp.1-15.
- [11] P. Liu, “A Computational Hydrodynamics Method for Horizontal Axis Turbine, Panel Method Modeling Migration from Propulsion to Turbine Energy”, Energy. 2010, Vol. 35, pp. 2843-2851.
- [12] I. H. Abbott and A. E. Von Doenhoff, Theory of Wing Sections, Dover Edition, New York (1959), pp. 110-187 and 536-537.
- [13] B. Multon, Energies Marines Renouvelables, Lavoisier Edition, Paris (2011), pp. 277-281.